

ARN

**JOURNAL OF
ENGINEERING
AND
APPLIED
SCIENCES**



**Dedicated to
the international of
engineering and technology**

**Volume 16
Number 13
July 2021
ISSN 1819-6608**

Published by

**Asian Research Publishing Network
Islamabat, Pakistan
www.arnjournals.com**

Editorial Board

Editor-in-Chief: Engr. J. K. Tarakzai (PAKISTAN)

Editors		Country
1	Prof. Dr. R. J. Godwin	UNITED KINGDOM
2	Prof. Dr. Erik Valdemar Cuevas Jimenez	GERMANY
3	Prof. Dr. Hamou SADAT	FRANCE
4	Dr. Mohammad Aminul Islam	JAPAN
5	Prof. Dr. Kui Fu Chen	CHINA
6	Prof. Dr. M. Ashraf Chaudhry	NEW ZEALAND
7	Prof. Dr. A. Sermet Anagun	TURKEY
8	Prof. Dr. Ashraf Mohamed Hemeida	Saudi Arabia
9	Prof. Dr. Krishna Murari Pandey	INDIA
10	Prof. Dr. Magdy A. Ezzat	EGYPT
11	Prof. Dr. Roberto Brighenti	ITALY
12	Dr. Anurag Misra	INDIA
13	Prof. Dr. Adel M. ALIMI	TUNISIA
14	Prof. Dr. Arun Kumar Gupta	INDIA
15	Prof. Demetrios V. Bandekas	GREECE
16	Prof. Dr. Bensafi Abd-El-Hamid	ALGERIA
17	Dr. Rajanish K. Kamat	INDIA
18	Prof. Dr. Asma Thamir Ibraheem	IRAQ
19	Prof. Dr. Sylejman Hyseni	KOSOVO
20	Prof. Dr. Haider Zaman	Saudi Arabia
21	Prof. Dr. Debojyoti Mitra	INDIA
22	Prof. Dr. Pandian VASANT	MALAYSIA
23	Prof. Dr. Prakash MMS Kinthada	INDIA

Associate Editors		Country
1	Dr. Dongning Li	USA
2	Dr. Suheyly Yerel	TURKEY
3	Dr. Guoxiang Liu	USA
4	Dr. Nadeem Anjum	PAKISTAN
5	Engr. Malini Sarah Philip	NORWAY
6	Dr. K.V.L.N. Acharyulu	INDIA
7	Engr. Mohammad Khalily Dermany	IRAN

8	Dr. Lamyaa- Gamal Eldeen Taha	EGYPT
9	Dr. OM Prakash Singh	INDIA
10	Engr. Seyyed Mohammad Reza Farshchi	IRAN
11	Dr. Muhammad Imran Din	PAKISTAN
12	Dr. José Carlos Páscoa Marques	PORTUGAL
13	Engr. Fawwaz Jinan Jibrael Jabri	IRAQ
14	Dr. Kanad Ray	INDIA
15	Dr. Shamsuddin Shahid	MALAYSIA
16	Engr. Naveenji Arun	INDIA



Table of Contents

ARPN Journal of Engineering and Applied Sciences

July 2021 | Vol. 16 No. 13

Numerical simulation of forced convective flows over a pair of side-by-side heated circular cylinders O. M. Oyewola, P. M. Singh, O. S. Ismail and K. Abu	1
A simulation model for the effect of resource consumption attack over MANET Raed Alsaqour, Maha Abdelhaq, Njoud Alghamdi, Maram Alneami, Tahani Alrsheedi, Salma Aldghbasi, Rahaf Almalki and Sarah Alqahtani	12
Analysis for the reinforced beam-column joint subjected to cyclic loading using ABAQUS and deep learning with python Maram Al-kisswani and Faidhi Alubaid	20
Model-View-Controller architecture on a programmable logic controller: Experiment with microalgae Claudia Lorena Garzón-Castro, Luis Beltrán, César Forero, María Loeber and Santiago Santacruz	39
The effect of production parameters on DC Thermal Plasma nanomaterial synthesis Salahuddin Junus, Fabrobi Ridha, Robertoes Koekoeh K. W. and Agung Budi Cahyono	48
Optimization of rotary composting process in Indonesian tropical climate for household solid waste recycling Slamet Raharjo, Suci Wulandari, Widya Eryuningsih, Yenni Ruslinda, Rizki Aziz and Yommi Dewilda	53
Identify cropping patterns of Cihea Irrigation Area in Cianjur Regency West Java using MODIS image data Delvi Yanti, Tineke Mandang, Mohamad Yanuar Jawardi Purwanto and Mohamad Solahudin	60
Hooked ends steel fibers effects on energy absorption capacity of concrete	

Carlos Gaviria-Mendoza, Miguel Ospina-García and Ana Ortiz-Sandoval	68
Performance of the PV module under different shading patterns E. T. El Shenawy, O. N. A. Esmail, Adel A. Elbaset and Hesham F. A. Hamed	75
Analysis of fitness for service in dented pipes by means of finite elements: Study case Edwin Torres Díaz, Saúl Andrés Hernández Moreno, Edwin Rúa Ramírez, Bladimir Ramon Valencia and Gonzalo G. Moreno-Contreras	83
Identifying Robellini Palm growth stages through a convolutional neuronal network Fredys A. Simanca H., Jaime Alberto Paez, Jairo Cortés Méndez and Fabian Blanco Garrido	91
An effective hybrid classifier for breast tumor classification Sannasi Chakravarthy S. R. and Harikumar Rajaguru	101
Exploiting image processing to measure dimension of short distant objects Nadeem Mahmood, Kashif Rizwan, Saeed Ullah and Muhammad Yaqoob Koondhar	107



THE EFFECT OF PRODUCTION PARAMETERS ON DC THERMAL PLASMA NANOMATERIAL SYNTHESIS

Salahuddin Junus, Fabrobi Ridha, Robertoes Koekoeh K. W. and Agung Budi Cahyono

Department of Mechanical Engineering, University of Jember, East Java, Indonesia

E-Mail: salahuddin.teknik@unej.ac.id

ABSTRACT

The practical use of Alumina in various fields of engineering has become more in demand due to its properties to withstand high temperature, resist corrosion, and possess good hardness and strength. The synthesis of alumina nanoparticles is done by DC Thermal Plasma method where aluminum powder is flowed through oxygen gas to pass through arc in plasma torch so that primary particles are combusted and cause evaporation and crystallization to form alumina nanoparticles in particular phases. The XRD (X-Ray Diffraction) observation results showed variations in aluminum powder flow rate of 4.72, 5.90, 7.08 and 8.26 l/min with a processing time of 10, 20, 30, 40s. The alumina nanoparticles formed different dominant phases of γ -alumina and δ -alumina phases with intensities above $\geq 75\%$. SEM (Scanning Electron Microscope) observations of the alumina nanoparticles was used to characterize the resulting particle diameter, morphology and structure. The powder flow rate variation of specific process times produced different agglomeration, mean size and structure of the resulting alumina nanomaterial.

Keywords: alumina nanomaterials, dc thermal plasma, nanomaterial synthesis.

1. INTRODUCTION

Aluminum oxide is one of the most cost-effective structural engineering materials and is widely used as a choice for ceramic material. The raw materials for high performance ceramic materials can be produced easily and at affordable prices, resulting in good aluminium oxide (alumina) grades. In the industrial sector, more than 45 million tonnes of Al_2O_3 are produced and marketed around the world and around 1.5 million tonnes of Al_2O_3 are used as raw powder worldwide [1]. It is used in coating, synthesis, and sacrificial anodes. This alumina application is used because alumina is resistant to acids, alkalis and corrosion. It also has high hardness and high temperature resistance [2].

There are various methods in synthesizing alumina nanoparticles but one of the most effective ways in synthesizing the nanoparticles into different phases are by using the DC thermal plasma method. By this method, a variety of crystal structure can be produced which includes several crystal forms such as (α , θ , ϑ , and γ) alumina. The crystal growth process of the alumina occurs due to very high process temperatures which allows the formation of phase transitions due to the high cooling process in the reactor [3].

The growth of alumina crystals obtained in the DC thermal plasma method can be controlled by adjusting the oxygen flow rate, powder flow rate, processing time and current on a DC thermal plasma [4, 5]. Previous research resulted in a 21 nm θ -alumina phase obtained with an oxygen gas flow rate of 16.5 l / min and a powder flow rate of 7.08 l / min, a 32.15 nm size ϑ -alumina phase obtained with an oxygen gas flow rate of 16.5 l / min and an oxygen gas flow rate of 16.5 l / min. powder flow was 4.72 l / min, while γ -alumina size of 20.52 nm was obtained with an oxygen flow rate of 25.9 l / min and a carrier flow rate of 4.72 l / min [5]. Controlling the process parameters such as oxygen flow rate, carrier flow rate and

processing time parameters could be carried out to obtain the desired phases of alumina crystallization.

2. EXPERIMENTAL METHOD

A schematic diagram of the experimental setup is shown in Figure-1 below.

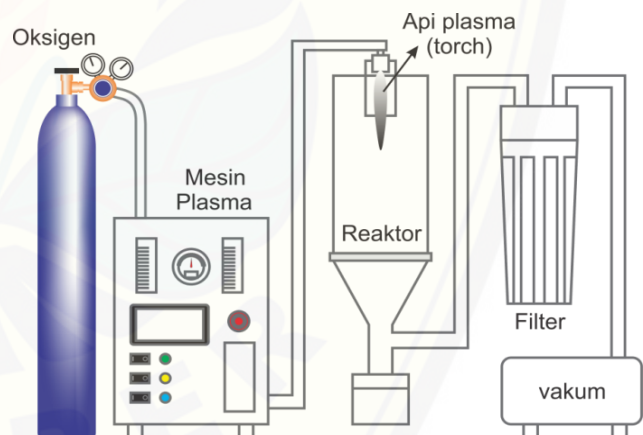


Figure-1. Schematic of DC thermal plasma synthesis device [6].

Alumina nanoparticles are formed in the reactor of the DC thermal plasma device due to the flow of oxygen gas with aluminum powder. A DC plasma torch is mounted on the head of the reactor where the precursor material and gas flow pass through the plasma flame. The plasma arc is achieved due to a short circuit between the anode and cathode which acts as the inner electrode and the outer electrode which is energized by plasma gas. Through the plasma, aluminum material changes from the solid phase to the liquid phase in this process due to high temperatures [4]. The particles will split and undergo evaporation and crystallization. The liquid phase will return to a solid phase and experience the formation of an



alumina nanoparticle phase [7]. The process of the alumina nanoparticle formation phase occurs during the crystallization process in the presence of temperature transformation.

During the experiment, precursor gas flow is set to a variation of (4.72, 5.90, 7.08 and 8.26) l/min. The precursor gas and plasma gas are O₂ with the plasma gas flow of 25.96 l/min. Processing time of (10, 20, 30, 40) seconds is conducted during the nanoparticle synthesis. The processing time considered is the time when the DC thermal plasma machine (DC Rillon Cutting 40) with current of 20A is activated and the precursor gas and material are fed into the reactor. Samples are collected through nanoparticle filters which is helped by a vacuum machine. All of the experiments are conducted in 1 atm.

Characterisation of materials are done using scanning electron microscope and XRD in Materials and Metallurgy Laboratory, Faculty of Industrial Engineering, Sepuluh November Institute of Technology, Surabaya. The Sem microscopy observation would be used for understanding the morphology of the resulting samples. These observations were made at variations in the flow rate of carrier gas 4.72 l / min and 8.26 l / min as well as variations in the processing time of 10 seconds and 40 seconds at 20,000x and 30,000x magnification using SEM device INSPECT S550. The XRD were carried out using the X'Pert Pro to understand the phase of the alumina samples. The result of XRD data on alumina nanoparticles with copper electrodes is then processed using MDI Jade 6 and Origin software.

3. RESULT AND DISCUSSIONS

The particle carrier flow rate plays an important role in the ignition of the plasma arc and plays a role in the length of time aluminum particle stays in the plasma flame [5]. Plasma flame is very influential in the process of alumina nanoparticles production because the plasma flame at a certain temperature is where carrier particles are formed to become alumina particles, resulting in the size of the alumina nanoparticle diameter [7]. This carrier flow rate acts as a driving force for aluminum to move towards the plasma flame torch. The more increasing of the carrier flow rate, the more aluminum powder carried on the plasma flame torch. This affects the aluminum powder feedrate and the production rate of alumina nanoparticles. The variation of processing time has a role in the duration of ignition of the plasma flame. The duration of the plasma flame during the manufacturing process greatly affects the rate of agglomeration in the alumina nanoparticles [8]. This can be seen from the following observations

SEM OBSERVATIONS

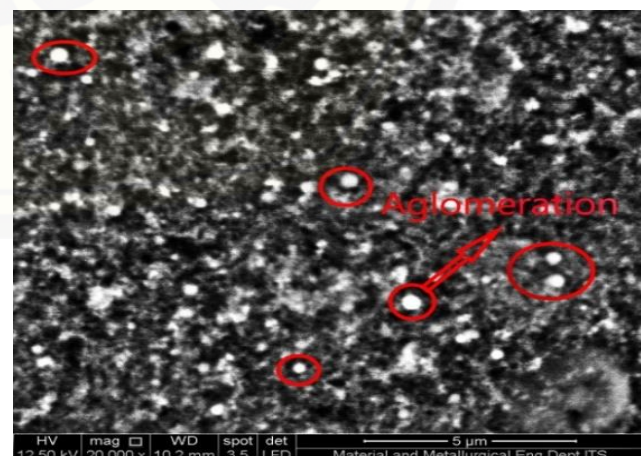
DC thermal plasma method alumina diameter SEM results from processing time of 40 seconds are shown in the table below. At carrier flow rate of 4.72 and 8.26 l / min show that alumina nanoparticles have a nanometer scale size of 14.57-43.71 nm and 14.57-56.64 nm respectively. The size of the alumina nanoparticle diameter is influenced by oxygen flow rate and the processing time used where the faster it leaves the plasma

flame, the smaller the particle diameter size. In this variation the alumina nanoparticles also experience a slight dominant agglomeration [7]. The size of the alumina nanoparticle diameter is influenced by the carrier oxygen flow rate and the processing time where the longer it leaves the plasma flame, the larger the particle diameter size will be [8]. This can result in the large amount of powder carried by oxygen into the plasma flame due to the high flow. So, when the aluminum powder enters the liquid phase to the solid phase, irregular agglomeration occurs.

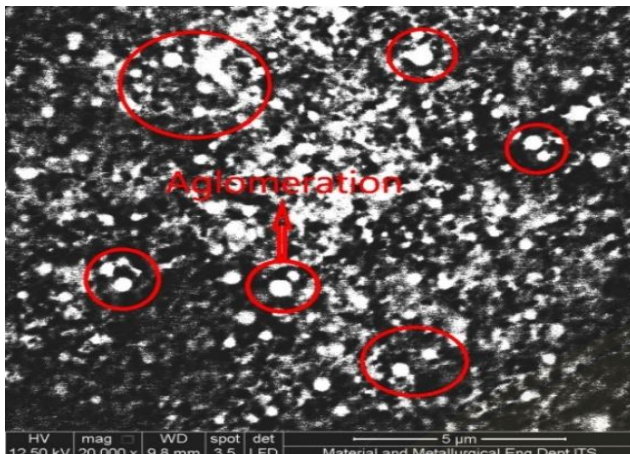
Table-1. Comparison of diameters of different carrier gas flow rate.

Gas Flow Rate (l/min)	Carrier Gas Flow Rate (l/min)	Current (A)	Process Time (s)	Average Diameter (nm)
25.96	4,72	20	40	14.57 – 43.71
25.96	8,26	20	40	14.57 – 56.64

The results of Table-4.1 SEM testing above show that the higher the flow rate of carrier rate and processing time can result in an enlargement of the diameter size of the alumina nanoparticles where the average diameter of the alumina. This occurs as particles experiences agglomeration at the increase in the variation of flow rate of carrier gas and processing time. This is due to the high temperature of the plasma flame during the process so that the precursor material leaves the plasma flame for too long and causes the materials to undergo an evaporation process for a longer time which causes the alumina nanoparticles to experience agglomeration [9]. The agglomeration formation at the variation of the flow rate of carrier gas 4.72 l / min at a processing time of 10 seconds and flow rate of 8.26 l / min at 40 seconds can be seen in the Figure-2 below.



(a)



(b)

Figure-2. Comparison of SEM observations of alumina nanoparticles (a) 4.72 l / min (b) 8.26 l / min.

It can be seen that the main occurrence of agglomeration is at the variation of carrier rate of 8.26 l / min and processing time of 40 seconds. Whereas at the variation of the rate of 4.72 l / min and a processing time of 10 seconds, the alumina particle size was evenly distributed and there were less alumina particles that experienced agglomeration. This is due to the accumulation of primary particles with other primary particles which results in increasing the size of the alumina nanoparticles.

XRD ANALYSIS

The highest intensity peak of alumina nanoparticles is located to determine the formation of phases and crystal structures formed from alumina nanoparticles. From Figure-3 (a) carrier rate of 4.72 l/min and 40s process time shows that the dominant alumina compound belongs to the Fd3m space group category with a peak intensity of 97% and has a cubic crystal structure. According to [10] the Fd3m space group is an alumina with a γ -alumina phase. This phase is formed at a temperature of 400-700°C [10]. The formation of the alumina phase is due to the reaction of liquid vapor when the aluminum particles undergo evaporation so that

oxidation occurs to form aluminum oxide and a fast quenching process occurs [11].

XRD results for carrier rate of 5.90 l/min and 40s process time is shown in Figure-3 (b). It shows that the dominant alumina compound belongs to the Fd3m space group category with a peak intensity of 86% and a cubic crystal structure at the variation of the flow rate of aluminum powder 5.90 l / min. According to research [10] the Fd3m space group is an alumina with a γ -alumina phase. This phase is formed at a temperature of 400-700°C [10]. The formation of the γ -alumina phase is due to the high flow rate of oxygen so that aluminum particles pass through the plasma flame quickly and quickly get a quenching treatment which results in a significant decrease in temperature [12].

Carrier rate of 7.08 l / min and processing time 40 seconds XRD results are shown in Figure-3 (c). that the dominant alumina compound falls into the P222 space group category with a peak intensity of 95% and an orthorhombic crystal structure at a variation of the aluminum powder flow rate of 7.08 l / min with a processing time of 40 seconds. In this case, according to research by [10] space group P222 is an alumina with a δ -alumina phase which is formed at temperatures of 800-900°C [13]. The formation of δ -alumina is due to temperature transformation in the formation of γ -alumina crystals into δ -alumina phases where these two phases are metastable phases so that crystal growth occurs rapidly [11].

The XRD results of the carrier rate of 8.26 l / min and a processing time of 40 seconds is explained in Figure-3 (d)., it shows that the dominant alumina compound belongs to the F-4m2 space group with a peak intensity of 75% and a tetragonal crystal structure at a variation of the flow rate of aluminum powder 8.26 l / min with a processing time of 40 seconds. In this case, according to research by [10] space group P222 is an alumina with a δ -alumina phase which is formed at a temperature of 800-900°C [13]. The formation of δ -alumina is due to temperature transformation when the particles occur in a cooling process, resulting in a direct nucleation process with very high crystal growth [14].

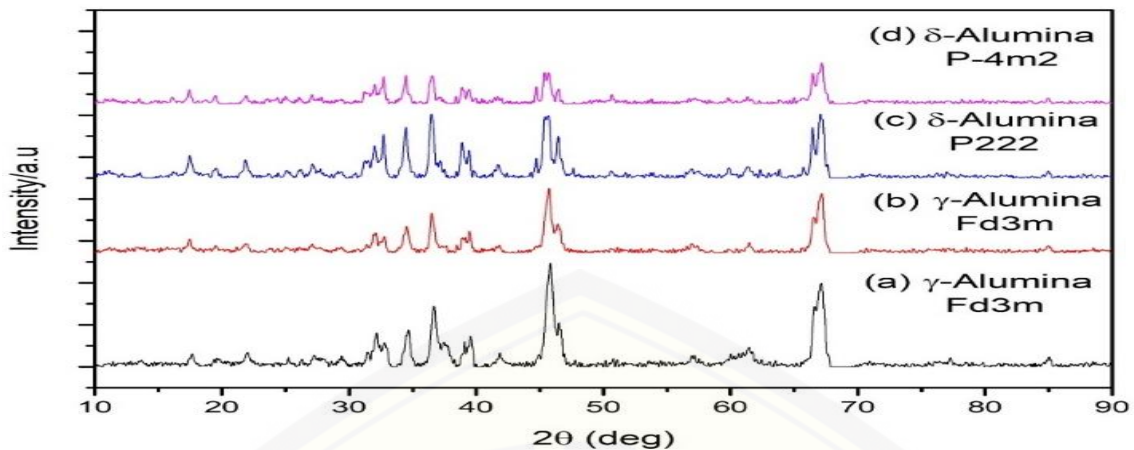


Figure-3. XRD observation results of alumina nanoparticles synthesized in 40s processing time with carrier of (a) 4.72 l / min, (b) 5.90 l/min, (c) 7.08 l/min and (d) 8.26 l / min.

The observational data can be compiled into a table below.

Table-2. Comparison of space group, phase and intensity of the resulting synthesis of different carrier gas flow rates.

Carrier Gas Flow Rate (l/min)	Process Time (s)	Space Group	Phase	Intensity (%)
4.72	40	Fd3m	γ-Alumina	97
5.90	40	Fd3m	γ-Alumina	86
7.08	40	P222	δ-Alumina	95
8.26	40	P-4m2	δ-Alumina	75

The table shows that there is a decrease in peak intensity at each increasing variation. In this case it can be seen that the effect of the increasing carrier flow rate and the longer processing time results in a decrease in the peak intensity of crystal phase formation in alumina nanoparticles and also experiences differences in space groups with the same phase at variations in carrier flow rate of 7.08 l / min and 8.26 l / min with a processing time of 40 seconds.

3. CONCLUSIONS

Based on the test results regarding the synthesis and characterization of alumina nanoparticles with variations in powder flow rate and processing time in the DC thermal plasma method, it can be concluded that there is a high level of agglomeration with the highest at the carrier flow rate of 8.26 l / min with a processing time of 40 seconds. It also has a larger diameter average diameter range of 14.57-56.64 nm. While at 4.72 l / min with a processing time of 10 seconds, it has the lowest agglomeration level. The average size of alumina particles produced also differs in the range of 14.57-43.71 nm.

XRD observations on the flow rates of carrier rate of 4.72 l / min and 5.90 l / min produce γ-alumina phase while at the flow rates of carrier rates 7.08 l / min and 8.26 l / min produce δ-alumina phase. The observations also show that on the carrier rate of 8.26 l / min produce a peak intensity of ≥75% while at a flow rate of 4.72 l / min it produces a high intensity peak with a percentage of ≥80%.

ACKNOWLEDGEMENTS

This work and publication is funded by the Ministry of Education and Culture of the Republic of Indonesia and University of Jember.

REFERENCES

- [1] Takashi Shirai *et al.* 2009. Structural Properties and Surface Characteristics on Aluminum Oxide Powders. Ceramics Research Laboratory 1.
- [2] A. I. Y. Tok, F. Y. C. Boey, X. L. Zhao. 2006. Novel synthesis of Al₂O₃ nano-particles by flame spray pyrolysis. Elsevier. 1.
- [3] B. Bora, et al. 2012. Free-flowing, transparent γ-alumina nanoparticles synthesized by a supersonic thermal plasma expansion process. Elsevier. 1.
- [4] Dirgantara A. G. 2016. Pengaruh Laju Aliran Partikel Aluminium Terhadap Pembentukan Nanopartikel Alumina dengan menggunakan Metode DC Thermal Plasma . 19.
- [5] Rochman, H. A. 2017. Pengaruh Laju Aliran Oksigen pada DC Thermal Plasma Terhadap Karakteristik Nanopartikel Alumina. 61.
- [6] Salahuddin Junus, Sumarji, Haidzar, Robertus Sidartawan. 2019. ARPN Journal of Engineering and Applied Sciences. 45.



- [7] K. P. Jayadevan dan T. Y. Tseng. 2004. Oxide Nanoparticles. Taiwan: ENN-Encyclopedia of Nanoscience and Nanotechnology.
- [8] R. Ye, J.-G. Li, T. Ishigaki. 2007. Controlled synthesis of alumina nanoparticles using inductively coupled thermal plasma with enhanced quenching. Elsevier. 6.
- [9] C. Chazelas *et al.* 2007. Synthesis of nanometer alumina particles by plasma transferred arc alternative. ELSEVIER. 3.
- [10] Jitendra Gangwar *et al.* 2015. Phase dependent thermal and spectroscopic responses of different morphogenesis of Al₂O₃ nanostructures. Nanoscale. 7.
- [11] K. Suresh, V. Selvarajan, M. Vijay. 2008. Synthesis of nanophase alumina, and spheroidization of alumina particles, and phase transition studies through DC thermal plasma processing. Elsevier. 1.
- [12] B. Bora, *et al.* 2012. Free-flowing, transparent γ -alumina nanoparticles synthesized by a supersonic thermal plasma expansion process. Elsevier. 1.
- [13] Metson J. 2011. Production of alumina. New Zealand: Woodhead Publishing Limited.
- [14] S. Kumar, *et al.* 2008. Synthesis and characterization of alumina nano-powders by oxidation of molten aluminium in a thermal plasma reactor: Comparison with theoretical estimation. Elsevier. 4.